PAPER

Check for updates

Accelerated degradation of Pt-coated Ti porous transport layers under dynamic potential pulses in PEMWEs†

Jeongah Lee,‡[a] Seongwoo Nam,‡[b] Hyunseung Kim, [b] Pilyoung Lee,[c] Soobin Yoon,[c] Young-June Park*[c] and WooChul Jung [*ab]

Proton exchange membrane water electrolyzers are vital for sustainable hydrogen production, but a lack of understanding of their durability under potential perturbation presents a significant challenge. This study investigates the degradation behavior of Pt-coated Ti-based porous transport layers (PTLs) under dynamic potential pulses, mimicking potential perturbation. Using a three-electrode system, anodic potential pulses alternating with open-circuit voltage are applied to the PTL, revealing severe degradation compared to constant potential application. The pulsed potential accelerates Pt dissolution through repeated electrochemical and chemical reactions, forming oxidized Pt species and causing coating detachment. Physicochemical analyses confirm increased Pt oxide formation and substantial coating layer desorption under pulsed conditions, resulting in a significant drop in electrical conductivity. PEMWE full-cell tests demonstrate that degraded PTLs led to increased overpotentials and reduced cell performance. This study highlights the critical impact of fluctuating potential on PTL durability, providing insights into enhancing the stability and performance of the water electrolyzer.

Introduction

Proton exchange membrane water electrolyzers (PEMWEs) are advanced energy conversion devices capable of producing high-purity green hydrogen with exceptional efficiency.[1–5] As the global demand for sustainable energy solutions grows,[6–10] PEMWEs are gaining attention for their potential to drive the hydrogen economy forward. However, one critical challenge to their widespread adoption lies in the effects of potential perturbation, which significantly impacts both the performance and durability of PEMWEs during operation.[11–13]

Potential perturbation refers to fluctuations in the current density caused by changes in power supply or demand, and it can lead to the degradation of various components in the PEMWE system. Among these components, the porous transport layer (PTL) plays a crucial role in facilitating reactant transport, ensuring proper water and gas management, and maintaining electrical conductivity.[14–18] Deterioration of

transport layers under dynamic operating conditions can compromise the overall system by reducing efficiency, increasing mass transport resistance, and accelerating mechanical wear.[19–21] Addressing these challenges is imperative to achieve the high durability required for commercial-scale applications of PEMWEs.[22,23] Despite its importance, studies focusing on the effects of fluctuating potential on the PTL remain scarce, especially compared to the well-documented impacts on electrocatalysts and the strategies to mitigate such degradation. Particularly in the chlorine evolution reaction (CER), which also accompanies anodic potential and acidic environment, several studies have reported the deactivation phenomena of noble metal catalysts under various dynamic potential conditions.[24–29] However, research on catalyst degradation under square-type potential pulse conditions is still limited, emphasizing the importance of examining the influence of abrupt potential changes on material durability. In this context, a deeper understanding of how potential perturbations affect the PTL is considered necessary.

This study aims to investigate the degradation behaviors of the widely adopted noble metal-coated Ti-based transport layers under potential perturbation. Notably, a Pt-electroplated PTL is utilized. Electroplating was selected over physical and spray coating methods due to its simplicity, cost-effectiveness, and suitability for large-scale fabrication.[30–33] Unlike other approaches, electroplating does not require a vacuum environment and enables uniform Pt deposition even within the complex porous structure of the PTL. Given the high material

[a]Department of Materials Science and Engineering, Seoul National University, Seoul 08826, Republic of Korea. E-mail: wcjung@snu.ac.kr

[b]Research Institute of Advanced Materials, Seoul National University, Seoul 08826, Republic of Korea. E-mail: wcjung@snu.ac.kr

[c]Hydrogen and Fuel Cell Development Center, Hyundai Motor Group, Yongin 16891, Republic of Korea. E-mail: yjpark2935@hyundai.com

† Electronic supplementary information (ESI) available. See DOI: https://doi.org/10.1039/d5ta00960j

‡ Jeongah Lee and Seongwoo Nam contributed equally to this study.

This journal is © The Royal Society of Chemistry 2025

J. Mater. Chem. A, 2025, **13**, 13495–13502 | **13495**

costs associated with PEM electrolyzers, a scalable and efficient coating method like electroplating is particularly advantageous. Additionally, while various alternative materials have been investigated for PTL coatings—including Ir-based catalysts, gold, and non-noble compounds like TiC and TiN—each presents significant drawbacks such as higher cost, limited availability, insufficient durability, or unproven long-term stability.[34,35] In contrast, Pt remains the most practical choice due to its well-established electrochemical performance and reasonable durability under harsh anode conditions, making it a reliable coating material for this study.[36]

To simulate potential perturbation on Pt-coated Ti PTLs, anodic potential is applied in a pulsed form using a three electrode system, followed by physicochemical and electrochemical characterization including scanning electron microscopy (SEM), X-ray diffraction (XRD), X-ray photoelectron spectroscopy (XPS), linear sweep voltammetry (LSV), and PEMWE single cell test. A significantly higher level of degradation was observed in the PTL subjected to potential pulses than in continuous potential, as confirmed by both the three electrode measurements and single cell tests. This was found to originate from the repeated dissolution of Pt, leading to the formation of oxide species generated from the coating layer. Our finding highlights that degradation under fluctuating potential is a critical challenge that cannot be overlooked and must be mitigated to achieve robust PEMWEs. By identifying the specific effects of dynamic operating conditions on transport layers, we provide insights into improving PEMWE durability and advancing their commercial viability as a sustainable hydrogen production technology.

Results and discussion

Potential pulses under three electrode system

We aimed to investigate the effect of power fluctuation on the PTL of the proton electrolyte membrane water electrolysis (PEMWE) cells (Fig. 1a). A Pt-coated Ti PTL was utilized, comprising a commercial powder-type Ti sheet with a thickness of approximately 260 μm, coated with approximately 0.35 μm of Pt *via* electroplating (Fig. S1†). The electroplating included control on the duration of the electrochemical deposition and current density, referring to a previous literature.[37] As shown in the SEM image, Ti metal powder were sintered in a thin sheet with high porosity for effective diffusion of oxygen gas (Fig. 1b). The spherical particles on the sheet are coated Pt, with the coating layer having a thickness equivalent to one to two particles. The thin coating was intentionally designed to minimize Pt usage for economic efficiency. The Pt nanoparticles are uniformly distributed on the Ti surface, with no significant defects observed, spanning from the outer regions to the inner regions of the PTL. The damage to the Pt coating layer directly triggers the exposure of Ti to the electrolyte, oxidation of Ti into titanium oxide, and subsequent decrease in electrical conductivity of the whole porous transport layer. Therefore, the corrosion of Pt is thoroughly explored in this study to gain insight into the stability of the PTL.

It is well established that in the anodic and acidic environments, the behavior of Pt significantly depends on the applied voltage.[38–40] Under a moderate oxidizing potential, Pt is easily oxidized to an ionic state, dissolving into the electrolyte; however, at very high oxidation voltages, it can undergo a phase transformation into an oxide. These intrinsic properties of Pt make it necessary to accurately control the applied potential to investigate its stability-related behavior. However, most of the previous literature on PTL with Pt only utilize single cell experiments.[30,41,42] Since the resistances across an electrolysis cell vary depending on the cell components, the applied voltage differs, and it is hard to identify the voltage corresponding to only PTL.[36] This issue can be addressed by utilizing a three electrode system with PTL as a working electrode, where the potential on the working electrode can be precisely controlled (Fig. 1c). Also, the start-up and shut-down, which is the representative dynamic condition in the cell can be mimicked by applying potential as pulses, alternating anodic potential and OCV (where a current value is zero). The application of pulse-type voltages can also be beneficial for effectively degrading Pt. Pt is known to exhibit transient properties for corrosion, where it favorably dissolves when potential is changed.[43–45] Therefore, it can be expected that the repetitive change in the voltage would not only trigger the oxidation of Pt into PtO_x or PtO_xH_y but also the dissolution of the oxidized Pt species. Also, the oxidized Pt species are reported to undergo severe chemical dissolution when the voltage applied decreases from the anodic potential to OCV.[46] The alternating anodic potential and OCV would much facilitate the dissolution of Pt. Therefore, applying potential pulses to the PTL using a three electrode system is considered a highly effective approach for investigating the degradation behavior, as it enables an accurate simulation of the situations observed within a PEMWE cell and accelerates the Pt coating deterioration.

Potential pulses-induced PTL degradation

Potential holds and potential pulses were each applied to the PTL, and the resulting degradation was examined. Potential holds refer to continuously applying 2.1 V_{RHE}, and potential pulses involve alternately applying 2.1 V_{RHE} and OCV, with each lasting for 5 seconds (Fig. 2a, S2 and S3†). Two kinds of potential were applied to the PTLs in 1 M H_2SO_4 electrolyte at 60 °C for 50 hours. The experimental conditions were determined to mimic the harsh operating condition of the PEMWE. The commercial cell typically operates within a voltage range of 1.8–2.0 V, and the catalyst–electrolyte interface experience significant decrease in local pH due to the oxygen evolution reaction.[47,48] Also, the operating temperature is generally between 50 to 80 °C, and the temperature was set to 60 °C considering the upward limit temperature of the reference electrode (Hg/Hg_2SO_4).[49] Although we employed conditions slightly harsher than typical operating environments to observe the effect of dynamic potential more rapidly and clearly, we ensured that the conditions remained within a realistic range for PEMWE systems.

13496 | *J. Mater. Chem. A*, 2025, **13**, 13495–13502
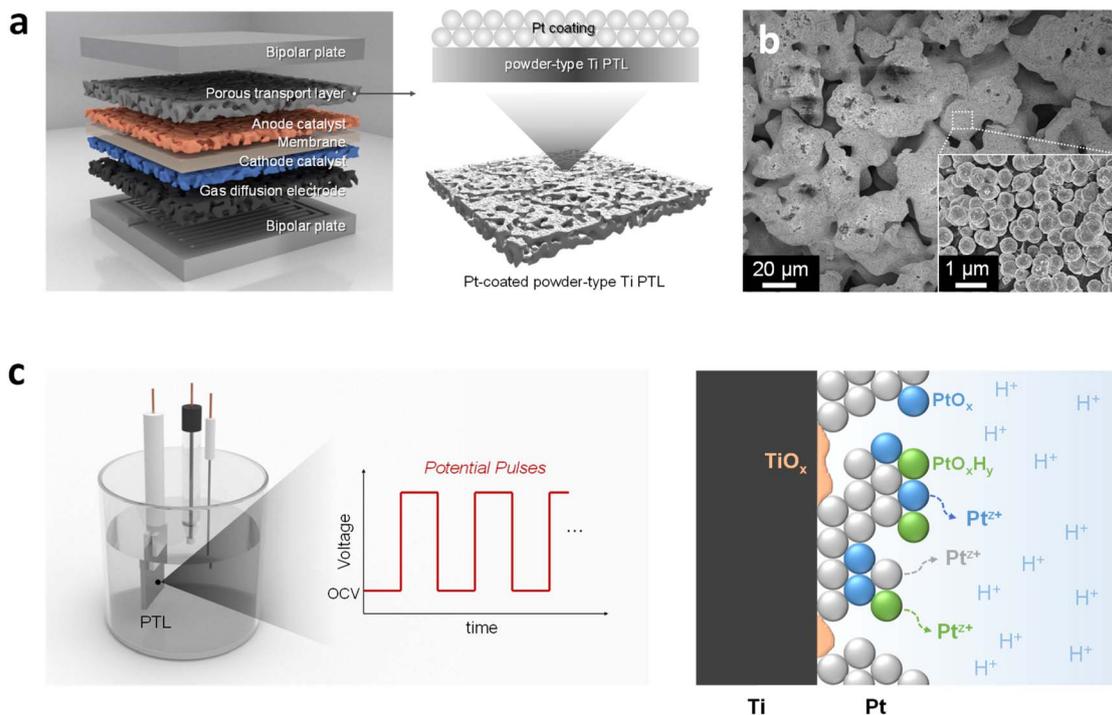
This journal is © The Royal Society of Chemistry 2025

Fig. 1 Potential pulses under three electrode system (a) schematic representation of PEMWE cell and Pt-coated Ti porous transport layer at the anode side. (b) SEM images of the porous transport layer used in this work. (c) Schematic representation of the three electrode setup with potential pulses* on the working electrode in H_2SO_4 aqueous solution, and the expected degradation of Pt coating and Ti during the potential pulses. *potential pulses: repetitive application of anodic potential and OCV alternatively.

The linear sweep voltammetry (LSV) curves in the anodic potential range were recorded in a forward scan before and after the operation to evaluate the degree of degradation (Fig. 2b). The measurements were conducted at 60 °C in 1 M H_2SO_4 electrolyte, and the potentials were converted into the reversible hydrogen electrode (RHE) scale. A prolonged exposure of Pt-coated Ti sheet to anodic potentials, the Ti surfaces in contact with the electrolyte become passivated with TiO_2.[50,51] As the insulating TiO_2 does not contribute to the oxidation current, Pt is the primary contributor to the LSV currents. According to the previous studies, Pt is active for the oxygen evolution reaction when in metallic state but becomes inactive in Pt oxide.[52] Furthermore, the detachment of the coating layer and the resulting formation of TiO_2 lead to a decrease in the electrical conductivity, also contributing to a downward shift of the curves. Therefore, the degree of Pt oxidation and the electrical conductivity decrease can be effectively evaluated through the LSV analyses, highly reflecting the degradation of the PTL. Comparing the LSV curves before and after the application of potentials, interestingly, while the curve did not change after the potential holds, the potential pulses for only 50 hours significantly decreased the currents. The overpotential value at 10 mA increased from 400 mV to 500 mV when subjected to the 50 hours of pulsed potentials. The significant increase in the overpotential suggests a notable increase in the resistance of the transport layer itself. Even applying an extremely high potential at harsh environments, the constant oxidation cannot effectively degrade the Pt. Consistent results were also observed

in the current pulses and holds test, further reinforcing the validity of our findings (see Fig. S4†). Considering the previous reports that demonstrate the extremely high stability for more than 500 hours of the Pt-coated Ti PTLs, the dynamic operation in our test have the potential to greatly corrode the resilient noble metal coating.[34,50]

The suggested scenario for the severe degradation under the potential pulses is described as a schematic illustration in Fig. 2c. As explained above, Pt undergoes dissolution when voltage increases and decreases, a process known as anodic dissolution and cathodic dissolution, respectively.[43–45] When the voltage increases from OCV to 2.1 V_{RHE}, anodic dissolution occurs as Pt metal oxidizes into its ionic form. Then, at 2.1 V_{RHE} for 5 seconds, Pt undergoes further oxidation, forming PtO_x or PtO_xH_y. When the voltage decreases to OCV, the oxidized Pt species are reduced and dissolved, and the subsequent serious chemical dissolution proceeds during the OCV.[46] Therefore, the application of potential pulses with oxidation potential and OCV facilitates the anodic and cathodic dissolution of Pt, the formation of Pt-oxidized species, and the chemical dissolution at the same time. Under a static oxidizing conditions, the metal surface would be passivated as metal oxide, so degradation is confined primarily to the outermost layer. However, the repeated dissolution of Pt *via* dynamic potential conditions exposes previously unoxidized regions of the Pt coating to the electrolyte, leading to continuous and accelerated degradation.
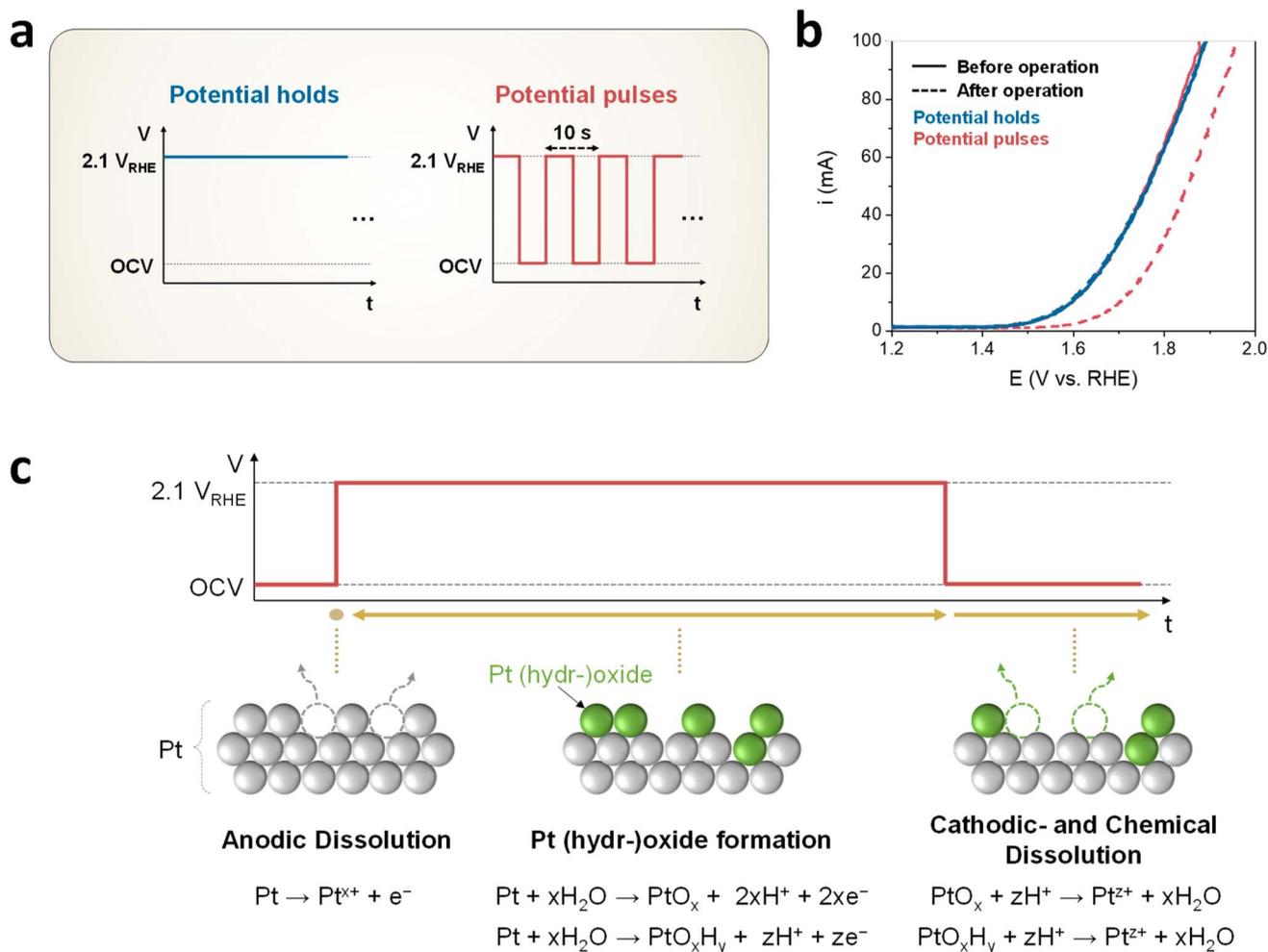
This journal is © The Royal Society of Chemistry 2025

J. Mater. Chem. A, 2025, 13, 13495–13502 | 13497

Fig. 2 Potential pulses-induced PTL degradation (a) schematic representation of the potential holds* and pulses tested in this work. (b) LSV curves for PTLs before and after 50 hours operation of potential holds and potential pulses. (c) Schematic illustration of the Pt coating degradation during the potential pulses. *potential holds: application of a constant anodic potential.

Effect of degraded PTL on PEMWE performance

To assess the impact of potential pulses on the practical full-cell performance, PTLs subjected to the potential holds and potential pulses for 50 hours in the previous section were mounted into the PEMWE cell, and the electrochemical performance was evaluated. The PTL was coupled with the IrO_2 as the anode and the gas diffusion electrode comprising of the gas diffusion layer and Pt/C were used as the cathode. The measurements were carried out at 65 °C with the flow of 75 mL min^{-1} at the anode side. In the polarization curves of the PEMWE cells, the cell with PTL exposed to potential pulses showed higher overpotential for the same current compared to that with PTL under potential holds (Fig. S5†). At a voltage of 2 V, the polarization curve for potential holds exhibited 3.34 A cm^{-2}, while that for potential pulses showed a significantly lower current density of 2.74 A cm^{-2}.

We conducted the electrochemical impedance spectroscopy for the PEMWE cells, from 1 kHz to 0.150 Hz (Fig. 3a and b). The spectra display an initial x-axis intercept, representing the ohmic resistance, along with two semicircles related to the

catalytic reaction at the anode and cathode. Since the transport layer contributes to the electrical contact of the cell components, the degradation would only affect the ohmic resistance. At both 1.25 A and 2.5 A, the cell with fresh PTL, PTL subjected to potential holds and pulses exhibited an ohmic resistance of approximately 126 mΩ cm^2, 129 mΩ cm^2 and 135 mΩ cm^2, respectively. We further measured the high frequency resistances of the two cells between 0.32 and 1 A (Fig. 3c). A similar trend was observed, where the cell with PTL subjected to potential pulses exhibited significantly increased high frequency resistance across all current values. The cell with the fresh PTL exhibited the lowest resistance, while the potential hold condition showed a slight increase, and the potential pulses resulted in the highest resistance. The relatively minor change after potential hold operation contrasts with the significant increase observed after pulses, indicating that the pulsed potential induces pronounced PTL degradation and corresponding performance loss. Additionally, evaluating the overall charge transfer resistances of the post-operation samples (Table S1†), the charge transfer resistance values of
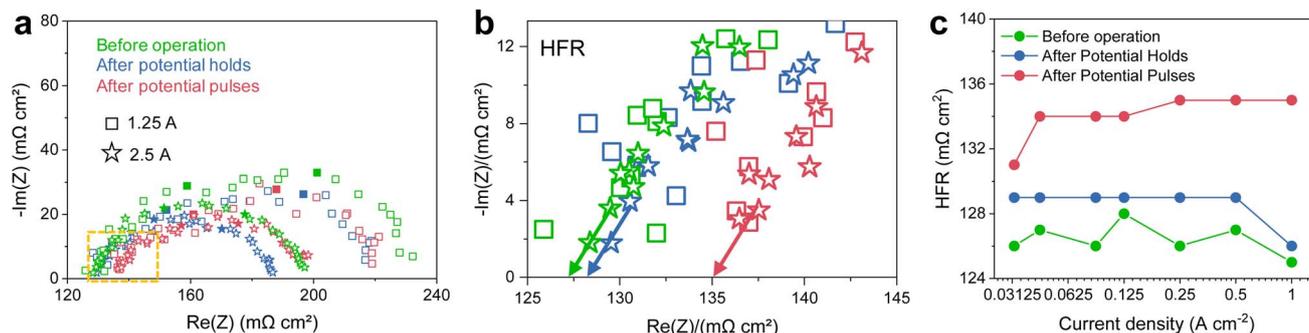
13498 | J. Mater. Chem. A, 2025, 13, 13495–13502

This journal is © The Royal Society of Chemistry 2025

Fig. 3 Effect of degraded PTL on PEMWE performance (a) EIS Nyquist plots of the PEMWE cells with PTLs before and after operation for 50 h. (b) The close-up of the high frequency resistance region in (a). (c) High frequency resistances of the PEMWE cells in (a).

the potential hold and potential pulse conditions are nearly identical. This suggests that PTL degradation did not significantly affect the catalyst's charge transfer kinetics. Thus, applying potential pulses for 50 hours can severely degrade the Pt coating and Ti substrate, leading to a noticeable increase in high frequency resistance and the reduction in the performance of the single cell. It also suggests a substantial impact of the PTL on the long-term stability of the PEMWE system.

Physicochemical analyses

To investigate the underlying reason on the significant degradation from the potential pulses, various physicochemical analyses were carried out on the PTLs under the operation of 50 hours in the previous section. X-ray diffraction (XRD) spectra show that the PTL subjected to potential pulses exhibit peaks for only Pt and Ti, while the PTL subjected to potential pulses displays an additional PtO_2 (011) peak (Fig. 4a). The presence of the oxide phase indicates an effective Pt oxidation under pulse operation. X-ray photoelectron spectroscopy (XPS) analyses of the Pt 4f spectra reveal that, after the potential holds, most of the surface Pt species remain as metallic Pt, whereas potential pulses significantly increase the ratio of PtO and PtO_2 on the surface (Fig. 4b and c). Additionally, we measured the open-circuit voltage (OCV) of PTLs after 50 hours of potential holds and potential pulses, respectively. Prior to measurement, the samples were conditioned by applying 2.1 V_{RHE} for 30 minutes to saturate the current. The inflection point observed in the OCV profile (Fig. S6†), which reflects the dissolution of PtO_xH_y, appeared later in the PTL subjected to potential pulses—indicating the presence of a larger quantity of partially oxidized Pt species. Furthermore, the stabilized OCV value was also higher for the potential pulses sample, suggesting a more oxidized surface state. It strengthens the result in X-ray-based analysis that surface oxidation was accelerated under the potential pulses.[46] It strengthens the result in XRD that surface oxidation was accelerated under the potential pulses. Scanning electron microscopy (SEM) analyses show that, in both PTLs, the Pt coating layer detached significantly, but with a much greater degree of detachment for the PTL subjected to potential pulses (Fig. 4d and e). It appears that in a harsh oxidizing environment, the Pt-coated Ti sheet experiences a peeling of the coating layer,

which directly exposes Ti to the electrolyte. And the application of potential pulses is much effective for the coating detachment, possibly leading to a larger area of exposed insulating TiO_2.

Notably, Ti is known for its natural tendency to form a stable oxide passivation layer upon exposure to oxygen or water, which contributes to its high corrosion resistance. This behavior is evident in the cyclic voltammetry (CV) results of the Pt-uncoated Ti PTL, where a sharp initial performance drops and the appearance of Ti oxide formation peaks were observed (Fig. S7†). This formation of Ti oxides is likely to have a direct and substantial impact on the decreased conductivity and performance of the PTL. Fig. S8† presents the Ti 2p XPS spectra of the PTLs after 50 hours of operation under both potential hold and pulse conditions. In both cases, the spectra are dominated by peaks assigned to Ti^{4+} species, indicating surface oxidation (TiO_2) of the Ti scaffold. Notably, the Ti 2p spectra of both PTLs are nearly identical, suggesting a comparable extent of Ti oxidation. This further underscores the fact that, despite similar levels of Ti oxide formation, the PTL subjected to potential pulses exhibited much more severe degradation. This finding highlights the more dominant role of Pt skin layer degradation, which underpins the central focus of our investigation.

The excessive formation of Pt oxide on the surface during potential pulses appears to be highly correlated with the coating peeling. We suggest that the Pt oxide formation at the defects of the coating layer weakens the binding strength between the coating layer and Ti, leading to the desorption of Pt. As the coating undergoes continuous oxidation, it eventually results in the detachment of large areas of the coating layer. Thus, applying pulsed voltage to a PTL promotes the formation of Pt oxide and accelerates the desorption of the coating layer compared to the constant voltage application. It significantly reduces the PTL's electrical conductivity and causes a deterioration in PEMWE full-cell performance due to an increase in high-frequency resistance. The discussion identifying the formation of oxidized species as a more critical factor than the electrochemical dissolution of Pt is presented in Fig. S9.†[53-56] Further research understanding the correlation between Pt oxide formation and coating layer desorption is required utilizing TOF-SIMS or STEM-EDS analyses.
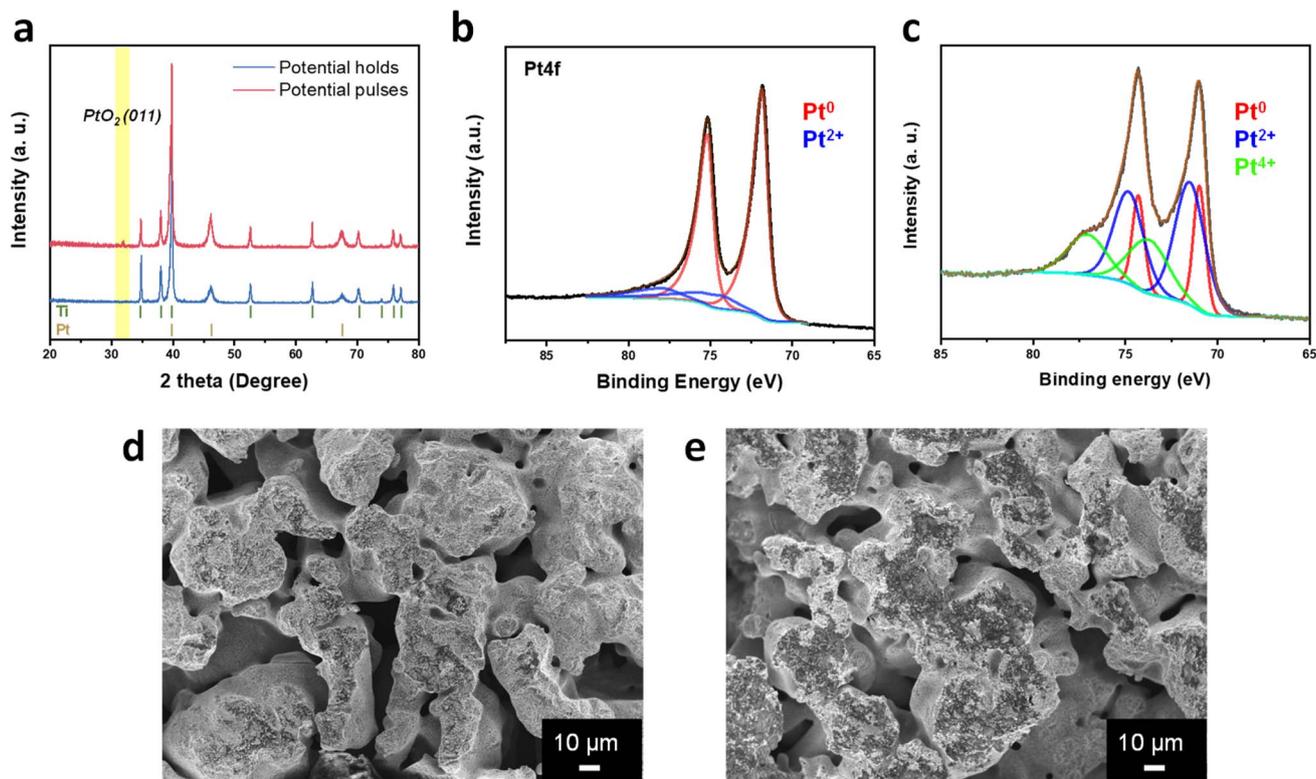
Fig. 4 Physicochemical analyses (a) XRD spectra for PTLs after operation of potential holds and pulses for 50 hours. Pt 4f XPS spectra of PTLs after operation of (b) potential holds and (c) potential pulses for 50 hours. SEM images of PTLs after operation of (d) potential holds and (e) potential pulses for 50 hours.

Conclusion

In conclusion, we unraveled that the potential pulses on the Pt-coated Ti transport layer of PEMWE significantly degrade the Pt coating and the overall cell performance. Utilizing a three electrode system, with the PTL as the working electrode, allowed for precise control over the voltage applied, leading to an accurate investigation of the electrochemical behavior. Due to the intrinsic properties of Pt, the dynamic potential induced the repetition of the electrochemical- and chemical dissolution of Pt and the formation of oxidized Pt species, leading to the severe Pt degradation. The PEMWE cell involving the PTL subjected to 50 hours of potential pulses exhibited a noticeable performance decline. Further physicochemical analyses revealed that transport layer under potential pulses contain an excessive amount of Pt oxide on the surface and the detachment of the coating layer. We suggest that the Pt oxide at the interface between the coating layer and Ti leads to the desorption of coating, exposing more Ti to the electrolyte, which significantly reduces the electrical conductivity. This study emphasizes the significant impact of fluctuating power on the degradation of the transport layer *via* systematic investigations. We anticipate our research to inspire follow-up studies exploring the PTL behavior under various extreme conditions, ultimately contributing to enhanced stability and performance of PEMWE system.

Experimental

Electrochemical characterization

The three-electrode system consisted of a Ti PTL as a working electrode, Hg/Hg_2SO_4 electrode as a reference electrode, and graphite rod as a counter electrode (see Fig. S2†). 1 M H_2SO_4 (ACS reagent, 95.0–98.0%, Sigma-Aldrich) aqueous solution was utilized as the electrolyte. Linear sweep voltammetry (LSV) was carried out in 1 M H_2SO_4 at 60 °C. The curves were forward-scanned with a sweep rate of 5 mV s^{-1} between 1.2 and 2.0 V_{RHE}. The potentials were converted into a reversible hydrogen electrode (RHE) scale using the eqn (1).

$$E_{RHE} = E_{Hg/Hg_2SO_4} + E^0_{Hg/Hg_2SO_4} + 0.59 \times pH \qquad (1)$$

PEMWE measurement

The catalyst layers of the PEMWE single cell consisted of IrO_2 (Boyaz Energy) for the anode and Pt/C (40 wt% Pt/C, Boyaz Energy) for the cathode, while the membrane employed was Nafion 115 (Dupont) with a thickness of 127 μm. Both catalysts were applied as catalyst coated membrane approach through decal-transfer method. The catalysts were first ultrasonically sprayed onto the polyimide film, and the films were hot-pressed onto the membrane at 120 °C with pressure of 55 kN and duration of 180 s.[57] The loading amounts were 4 mg cm^{-2} for

13500 | *J. Mater. Chem. A*, 2025, **13**, 13495–13502

This journal is © The Royal Society of Chemistry 2025

IrO_2 and 0.5 mg cm^{-2} for Pt/C. The membrane was conditioned before the cell construction through three steps as followed.

(1) Boiling at 80 °C in 3% H_2O_2 solution for 1 hour.

(2) Boiling at 80 °C in deionized water for 2 hours.

(3) Slightly boiling at 80 °C in 0.5 M H_2SO_4

The membrane was rinsed after each boiling step and it was stored in deionized water.

The test assembly consisted of a catalyst-coated membrane, a Pt-coated Ti porous transport layer, a gas diffusion layer, and anodized Al end plates. Ultrapure water was used as the electrolyte, and the active electrode area exposed to the electrolyte was 5 cm^2. The electrolyte flow rate was maintained at 75 mL min^{-1} on the anode side, and all measurements were conducted at 65 °C. After a stabilization period of 20 minutes, the polarization curve was recorded, with current values measured after each potential step maintained for 1 minute. The measurement was repeated five times, and the final curve was used for data analysis. Electrochemical impedance spectroscopy was performed over a frequency range of 1 kHz to 0.150 Hz.

Physicochemical characterization

The constituting crystalline phases of PTLs were analyzed through the X-ray diffraction (XRD, SmartLab, RIGAKU) analyses. The Cu Kα1 radiation was utilized with a Ge(111) monochromator. The chemical species of the surfaces of PTLs were probed by the X-ray photoelectron spectroscopy (XPS, K-alpha, Thermo VG Scientific). The scanning electron microscopy (SEM) analyses were carried out for the investigation of the surface morphologies of the PTLs (JSM-7600F, JEOL).

Data availability

The datasets used and/or analyzed during the current study are available from the corresponding author on reasonable request.

Conflicts of interest

The authors declare no conflict of interest.

Acknowledgements

References

1 R. Ram, L. Xia, H. Benzidi, A. Guha, V. Golovanova, A. Garzón Manjón, D. Llorens Rauret, P. Sanz Berman, M. Dimitropoulos, B. Mundet, E. Pastor, V. Celorrio, C. A. Mesa, A. M. Das, A. Pinilla-Sánchez, S. Giménez, J. Arbiol, N. López and F. P. García de Arquer, *Science*, 2024, **384**, 1373.

2 M. F. Lagadec and A. Grimaud, *Nat. Mater.*, 2020, **19**, 1140.

3 J. K. Lee, F. Babbe, G. Wang, A. W. Tricker, R. Mukundan, A. Z. Weber and X. Peng, *Joule*, 2024, **8**, 2357.

4 M. Carmo, D. L. Fritz, J. Mergel and D. Stolten, *Int. J. Hydrogen Energy*, 2013, **38**, 4901.

5 A. Buttler and H. Spliethoff, *Renewable Sustainable Energy Rev.*, 2018, **82**, 2440.

6 J. Kim, J. Lee, S. Kim and W. Jung, *Electron. Mater. Lett.*, 2024, **20**, 450–458.

7 S. Nam, J. Kim, H. Kim and W. Jung, *InfoScience*, 2024, 1.

8 H. Sun, X. Xu, H. Kim, Z. Shao and W. Jung, *InfoMat*, 2024, **6**, 1.

9 S. Nam, J. Kim, H. Kim, S. Ahn, S. Jeon, Y. Choi, B. Park and W. Jung, *Adv. Mater.*, 2024, 1.

10 S. Jeon, W. Jung, H. Bae, S. Ahn, B. Koo, W. Yu, S. Kim, D. Oh, U. Kim, S. A. Barnett, J. Seo, B. Kim and W. Jung, *Adv. Mater.*, 2024, 1.

11 J. Liu, L. Huang, J. Leveneur, H. Fiedler, S. Clarke, T. Larsen, J. Kennedy and M. Taylor, *J. Electrochem. Soc.*, 2024, **171**, 054521.

12 B. Xu, Y. Yang, J. Li, Y. Wang, D. Ye, L. Zhang, X. Zhu and Q. Liao, *Renewable Energy*, 2024, **232**, 121084.

13 H. Kojima, K. Nagasawa, N. Todoroki, Y. Ito, T. Matsui and R. Nakajima, *Int. J. Hydrogen Energy*, 2023, **48**, 4572.

14 S. H. Park, J. Koo, Y.-J. Park, S. Jang, H. J. Ryu, H. Han and K. T. Lee, *Chem. Eng. J.*, 2024, **481**, 148276.

15 J. Cho, D. H. Kim, M. W. Noh, H. Kim, H.-G. Oh, P. Lee, S. Yoon, W. Won, Y.-J. Park, U. Lee and C. H. Choi, *J. Mater. Chem. A*, 2024, **12**, 23688.

16 T. L. Doan, H. E. Lee, S. S. H. Shah, M. Kim, C. Kim, H. Cho and T. Kim, *Int. J. Energy Res.*, 2021, **45**, 14207.

17 Y. Tao, M. Wu, M. Hu, X. Xu, M. I. Abdullah, J. Shao and H. Wang, *SusMat*, 2024, **4**, 1.

18 Z. Kang, S. M. Alia, J. L. Young and G. Bender, *Electrochim. Acta*, 2020, **354**, 136641.

19 T. Schuler, J. M. Ciccone, B. Krentscher, F. Marone, C. Peter, T. J. Schmidt and F. N. Büchi, *Adv. Energy Mater.*, 2020, **10**, 1.

20 S. Stiber, H. Balzer, A. Wierhake, F. J. Wirkert, J. Roth, U. Rost, M. Brodmann, J. K. Lee, A. Bazylak, W. Waiblinger, A. S. Gago and K. A. Friedrich, *Adv. Energy Mater.*, 2021, **11**, 1.

21 C. Liu, M. Shviro, A. S. Gago, S. F. Zaccarine, G. Bender, P. Gazdzicki, T. Morawietz, I. Biswas, M. Rasinski, A. Everwand, R. Schierholz, J. Pfeilsticker, M. Müller, P. P. Lopes, R. Eichel, B. Pivovar, S. Pylypenko, K. A. Friedrich, W. Lehnert and M. Carmo, *Adv. Energy Mater.*, 2021, **11**, 2002926.

22 A. Lim, H.-Y. Jeong, Y. Lim, J. Y. Kim, H. Y. Park, J. H. Jang, Y.-E. Sung, J. M. Kim and H. S. Park, *Sci. Adv.*, 2021, **7**, 1.

23 X.-Z. Yuan, N. Shaigan, C. Song, M. Aujla, V. Neburchilov, J. T. H. Kwan, D. P. Wilkinson, A. Bazylak and K. Fatih, *Sustainable Energy Fuels*, 2022, **6**, 1824.

24 H. W. Lim, D. K. Cho, J. H. Park, S. G. Ji, Y. J. Ahn, J. Y. Kim and C. W. Lee, *ACS Catal.*, 2021, **11**, 12423.

25 A. B. Abdel-Aziz, F. E. T. Heakal, R. M. El Nashar and I. M. Ghayad, *Sci. Rep.*, 2024, **14**, 9821.

26 R. Manoharan and J. B. Goodenough, *Electrochim. Acta*, 1991, **36**, 19.

27 L. Liu, T. Dong, Y. Xin, Z. Ye, P. Zhao, W. Gao, H. Tang, T. Yin, Z. Ren and Y. Zhu, *New J. Chem.*, 2024, 17969.

This journal is © The Royal Society of Chemistry 2025

J. Mater. Chem. A, 2025, **13**, 13495–13502 | **13501**

28 N. Goudarzi, K. Jafarzadeh, A. Kashi and H. Mazhari Abassi, *Ionics*, 2023, **29**, 2351.

29 B. V. Tilak, V. I. Birss, J. Wang, C.-P. Chen and S. K. Rangarajan, *J. Electrochem. Soc.*, 2001, **148**, D112.

30 C. Liu, J. A. Wrubel, E. Padgett and G. Bender, *Appl. Energy*, 2024, **356**, 122274.

31 Z. Fan, H. Yu, G. Jiang, D. Yao, S. Sun, J. Chi, B. Qin and Z. Shao, *Int. J. Hydrogen Energy*, 2022, **47**, 18963.

32 T. L. Doan, H. E. Lee, M. J. Kim, W. C. Cho, H. S. Cho and T. Kim, *J. Power Sources*, 2022, **533**, 231370.

33 X. Wang, J. Zou, Z. Zhang, C. Zhao, M. Wang and M. Wu, *Fuel*, 2025, **381**, 133559.

34 C. Liu, M. Shviro, A. S. Gago, S. F. Zaccarine, G. Bender, P. Gazdzicki, T. Morawietz, I. Biswas, M. Rasinski, A. Everwand, R. Schierholz, J. Pfeilsticker, M. Müller, P. P. Lopes, R. Eichel, B. Pivovar, S. Pylypenko, K. A. Friedrich, W. Lehnert and M. Carmo, *Adv. Energy Mater.*, 2021, **11**, 2002926.

35 T. Deng, H. Huang, L. Fan, S. Xu and H. Li, *ACS Sustain. Chem. Eng.*, 2023, **11**, 17075.

36 B. Hasa, U. R. Aryal, S. Higashi, N. E. Tolouei, J. T. Lang, B. Erb, A. Smeltz, I. V Zenyuk and G. Zhu, *Appl. Catal., B*, 2025, **361**, 124616.

37 H.-Y. Jung, S.-Y. Huang and B. N. Popov, *J. Power Sources*, 2010, **195**, 1950.

38 D. J. S. Sandbeck, O. Brummel, K. J. J. Mayrhofer, J. Libuda, I. Katsounaros and S. Cherevko, *ChemPhysChem*, 2019, **20**, 2997.

39 R. Mom, L. Frevel, J.-J. Velasco-Vélez, M. Plodinec, A. Knop-Gericke and R. Schlögl, *J. Am. Chem. Soc.*, 2019, **141**, 6537.

40 K. Sasaki, N. Marinkovic, H. S. Isaacs and R. R. Adzic, *ACS Catal.*, 2016, **6**, 69.

41 S. Stiber, N. Sata, T. Morawietz, S. A. Ansar, T. Jahnke, J. K. Lee, A. Bazylak, A. Fallisch, A. S. Gago and K. A. Friedrich, *Energy Environ. Sci.*, 2022, **15**, 109.

42 A. Lim, J. Kim, H. J. Lee, H.-J. Kim, S. J. Yoo, J. H. Jang, H. Young Park, Y.-E. Sung and H. S. Park, *Appl. Catal., B*, 2020, **272**, 118955.

43 T. Fuchs, V. Briega-Martos, J. Drnec, N. Stubb, I. Martens, F. Calle-Vallejo, D. A. Harrington, S. Cherevko and O. M. Magnussen, *Angew. Chem.*, 2023, **135**, e202304293.

44 S. Cherevko, N. Kulyk and K. J. J. Mayrhofer, *Nano Energy*, 2016, **29**, 275.

45 A. A. Topalov, S. Cherevko, A. R. Zeradjanin, J. C. Meier, I. Katsounaros and K. J. J. Mayrhofer, *Chem. Sci.*, 2014, **5**, 631.

46 J. Cho, H. Kim, H.-S. Oh and C. H. Choi, *JACS Au*, 2023, **3**, 105.

47 J. Cho, D. H. Kim, M. W. Noh, H. Kim, H. G. Oh, P. Lee, S. Yoon, W. Won, Y. J. Park, U. Lee and C. H. Choi, *J. Mater. Chem. A*, 2024, 23688.

48 M. Carmo, D. L. Fritz, J. Mergel and D. Stolten, *Int. J. Hydrogen Energy*, 2013, **38**, 4901.

49 M. Bonanno, K. Müller, B. Bensmann, R. Hanke-Rauschenbach, D. Aili, T. Franken, A. Chromik, R. Peach, A. T. S. Freiberg and S. Thiele, *Adv. Mater. Technol.*, 2024, **9**, 1.

50 T. Srour, K. Kumar, V. Martin, L. Dubau, F. Maillard, B. Gilles, J. Dillet, S. Didierjean, B. Amoury, T. D. Le and G. Maranzana, *Int. J. Hydrogen Energy*, 2024, **58**, 351.

51 C. Rakousky, U. Reimer, K. Wippermann, M. Carmo, W. Lueke and D. Stolten, *J. Power Sources*, 2016, **326**, 120.

52 M. Favaro, C. Valero-Vidal, J. Eichhorn, F. M. Toma, P. N. Ross, J. Yano, Z. Liu and E. J. Crumlin, *J. Mater. Chem. A*, 2017, **5**, 11634.

53 X. You, J. Han, V. Del Colle, Y. Xu, Y. Chang, X. Sun, G. Wang, C. Ji, C. Pan, J. Zhang and Q. Gao, *Commun. Chem.*, 2023, **6**, 101.

54 R. Sharma, S. Gyergyek and S. M. Andersen, *Appl. Catal., B*, 2022, **311**, 121351.

55 R. M. Mensharapov, D. D. Spasov, N. A. Ivanova, A. A. Zasypkina, S. A. Smirnov and S. A. Grigoriev, *Inorganics*, 2023, **11**, 103.

56 D. J. S. Sandbeck, O. Brummel, K. J. J. Mayrhofer, J. Libuda, I. Katsounaros and S. Cherevko, *ChemPhysChem*, 2019, **20**, 2997.

57 A. M. Chaparro, R. Benítez, L. Gubler, G. G. Scherer and L. Daza, *J. Power Sources*, 2007, **169**, 77.

13502 | *J. Mater. Chem. A*, 2025, **13**, 13495–13502

This journal is © The Royal Society of Chemistry 2025